



A simplified model for inelastic behavior of an idealized granular material

Luigi La Ragione^{a,*}, Vincent C. Prantil^b, Ishan Sharma^c

^a *Dipartimento di Ingegneria Civile e Ambientale Politecnico di Bari, 70125 Bari, Italy*

^b *Department of Mechanical Engineering, Milwaukee School of Engineering, Milwaukee, WI 53202-3109, United States*

^c *Department of Mechanical Engineering, IIT Kanpur, Kanpur 208016, India*

Received 1 February 2007; received in final revised form 14 June 2007

Abstract

In this paper, our main interest is to describe the inelastic behavior of a granular material in the range of deformation that precedes localization. We do this in the simplest possible way, by idealizing the material as a random array of identical, elastic, frictional spheres and assuming that particles move with the average strain. The contact force is assumed non-central: the normal component follows the Hertz's law, while the tangential component is elastic until frictional-sliding occurs. We provide an analytical description of this material in triaxial extension and compression at fixed pressure, for both loading and unloading. We obtain expressions for the stress–strain relation, the plastic strain, the elastic and plastic volume change, the strain hardening and the potential function. We assume the Mohr–Coulomb criterion for yielding and we obtain an explicit expression between dilatancy and stress in the material.

© 2007 Elsevier Ltd. All rights reserved.

Keywords: Micro-mechanics; A. Yield condition; B. Granular Materials

* Corresponding author. Tel.: +39 080 5963739; fax: +39 080 5963719.
E-mail address: l.laragione@poliba.it (L. La Ragione).

1. Introduction

We study qualitative features of a granular material in the regime of deformation before the onset of localization. We want to focus on the mechanisms associated with the elastic and inelastic behavior in this range of deformation where it is reasonable to consider the average small strain response. Our interest is to develop the simplest micro-mechanical theory that helps us to understand how well-known macroscopic features are linked with the behavior at particle level. To this end we focus on a typical test for a granular material, loading and unloading the aggregate in triaxial compression and extension at fixed pressure. We assume that particles move according to the average strain, considering, therefore, the simplest possible approach to the problem. Although more accurate theories have been developed (e.g. Koenders, 1987; Misra and Chang, 1993; Jenkins, 1997; Liao et al., 1997) that include deviations from average fields, none of them have been employed to obtain analytical relations in the inelastic regime. Models employing numerical simulation to predict the inelastic behavior of a granular assembly far from its initial state have been proposed (e.g. Chang and Hicher, 2005; Nicot and Darve, 2006; Nicot et al., 2007). Continuum-level plasticity models, incorporating a fabric tensor to represent anisotropy have also been developed for general loading and unloading conditions (e.g. Nemat-Nasser and Zhang, 2002; Zhu et al., 2006a,b). Contributions have been also proposed to describe localization in granular material with gradient plasticity (e.g. Vardoulakis and Aifantis, 1991) and a decomposition of the inelastic stretching (e.g. Tsutsumi and Hashiguchi, 2005; Hashiguchi and Tsutsumi, 2007).

Here we develop a micro-mechanical approach that provides analytical results associated with dilatancy, plastic volume change and a plastic potential function. We anticipate that the analytical model will be justified over the narrow range of deformation in which elasticity and sliding among particles play the dominant role, rather than deletion and rearrangement of the particles in the aggregate.

Thornton and Antony (1998) have performed discrete element simulations of frictional, elastic spheres undergoing triaxial compression at fixed pressure in a periodic cell. Although their simulation is performed over a wide range of deformation, we concentrate our attention on loading that precedes the peak in deviatoric stress where the maximum amount of inter-particle contact sliding occurs. At this point, only approximately 10% of the average number of contacts per particle have been deleted. Moreover, particles whose contact have been deleted are those only weakly loaded in the initial isotropic compression. These contacts contribute predominantly to the mean stress and not the deviatoric stress. The anisotropy in the contact distribution, known as the aggregate fabric, is relatively small in the range of deformation of interest here.

Therefore, the assumption of only small deviations from an isotropic distribution of contacts is reasonable for the small strains considered here. Note, even after assuming an isotropic contact distribution, there is anisotropy of the response at the particle level as contact displacements and forces will be an explicit function of contact angle with respect to the principal direction of the applied compression.

In this context, a simplified model will provide qualitative description of the inelastic material behavior rather than quantitative predictions. In this way, we extend the salient results obtained by Jenkins and Strack (1993). These include analytical solutions at the aggregate level for the volume change, stress–strain response, and inelastic strain hardening for monotonic triaxial compression. We extend this work to include unloading and

reverse loading. Assuming negligible change in the orientational contact distribution, we derive an expression for the plastic volume change, the yield function based on the Mohr–Coulomb criterion and the plastic potential function (Nicot and Darve, 2007, have recently investigated the notion of the flow rule in the case of general loadings, including the triaxial test). For the small strains considered here, we anticipate that the dominant physical mechanisms that contribute to the dilatancy of the granular packing are the contact forces and frictional-sliding.

2. Theory

The granular material is idealized as a random array of identical elastic, frictional, spheres with diameter D , shear modulus G and Poisson's ratio ν . Jenkins and Strack (1993) provide analytical expressions for the stress–strain response, the volume change, plastic strain and strain hardening associated with contact sliding caused by monotonic triaxial compression at fixed pressure. We use part of their results and extend their applicability to both loading and unloading in axisymmetric extension and compression at fixed pressure.

2.1. Behavior at the particle contact level

2.1.1. Kinematics

Throughout this work, we adopt the same notation used in Jenkins and Strack (1993). Generally, in the presence of an evolution of the packing, it would be judicious to adopt an incremental formulation for any model describing inelastic response of the granular assembly. For sufficiently small deformations, however, where it is a reasonable assumption to consider the geometry of the packing fixed, integrations of incremental expressions for contact force, displacement and the average stress tensor are shown to be possible (Jenkins and Strack, 1993). Therefore, while many microstructurally-based models of inelastic response are necessarily incremental, the particular model developed by Jenkins and Strack (1993) with a continuous contact orientation field permits full integration and analytical expression in terms of total strain.

The displacement \mathbf{u} of a contact point relative to the particle center is written in terms of the average strain \mathbf{E}

$$u_i = \frac{D}{2} E_{ij} \alpha_j, \quad (1)$$

where $\boldsymbol{\alpha}$ is the unit vector directed from the particle center to the contact point. The rectangular Cartesian components of $\boldsymbol{\alpha}$ are $(\sin \theta \cos \varphi, \sin \theta \sin \varphi, \cos \theta)$, where θ is the polar angle from the axis of symmetry and φ is the angle about this axis (see Fig. 1).

The normal and tangential components of the contact displacement are, respectively:

$$\delta = \frac{D}{6} (\Delta - 2\gamma + 6\gamma \cos^2 \theta) \quad (2)$$

and

$$\mathbf{s} = D\gamma \sin \theta \cos \theta \mathbf{e}_\theta,$$

where \mathbf{e}_θ , with components $(\cos \theta \cos \varphi, \cos \theta \sin \varphi, -\sin \theta)$, is the unit vector in the direction of increasing θ . In the axisymmetric compression and extension, the volume strain Δ (taken positive for a decrease in volume) and the shear strain γ are, respectively:

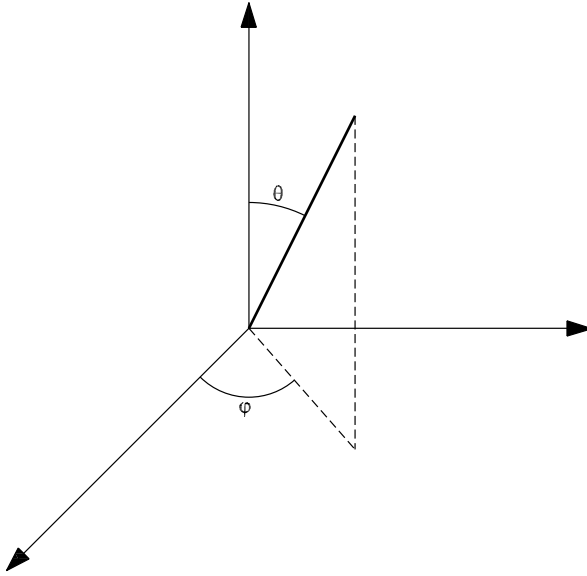


Fig. 1. Schematic representation of the contact direction with the angles θ and ϕ .

$$\Delta = -(E_{33} + 2E_{11})$$

and

$$\gamma = -\frac{1}{2}(E_{33} - E_{11}).$$

2.1.2. Contact force

The interaction between the particles is represented by a non-central force \mathbf{F} , which is comprised of a Hertzian normal contact force P , and an elastic frictional-sliding tangential contact force, \mathbf{T} . The particle contact force is then given by

$$F_i = P\alpha_i - T_i. \quad (3)$$

For the normal component, the relation between force and normal displacement δ is

$$P = M \left(\frac{6\delta}{D} \right)^{3/2}, \quad (4)$$

where $M = 2GD^2/[9\sqrt{3}(1-\nu)]$. For the tangential component, we assume an elastic, perfectly plastic, bilinear behavior. That is, the tangential response is linear elastic until $T = \mu P$, with μ the coefficient of friction, at which point the tangential force remains fixed and inelastic frictional-sliding occurs. We, therefore, adopt relatively simple models for the contact forces that are integrated solutions of a more elaborate contact law introduced by Mindlin and Deresiewicz (1953). An example of a more rigorous interpretation of the contact law has been furnished by Elata et Berryman (1996) and recently by Nicot and Darve (2005).

At sliding, the tangential elastic displacement reaches its limiting value (Jenkins and Strack, 1993)

$$s^{el} = \hat{\mu}\delta, \tag{5}$$

where $\hat{\mu} = \mu(2 - \nu)/(3 - 3\nu)$. So,

$$T = \begin{cases} Ks & \text{for } s \leq s^{el}, \\ \mu P & \text{for } s > s^{el}, \end{cases}$$

where $K = 2^{5/3}G^{2/3}[3(1 - \nu)DP]^{1/3}/(2 - \nu)$.

We note that in a triaxial test the tangential displacement is a monotonic function of the applied strain, while the normal component can increase or decrease during the loading.

2.2. Behavior at the aggregate level

2.2.1. Pressure and volume change

The average stress tensor is represented by (e.g. Love, 1942)

$$\bar{t}_{ij} = -\frac{nD}{2} \int_{\Omega} f(\boldsymbol{\alpha}) F_i \alpha_j d\Omega,$$

where $f(\boldsymbol{\alpha})d\Omega$ is the probable number of contacts within the solid angle $d\Omega = \sin \theta d\theta d\varphi$ centered at $\boldsymbol{\alpha}$ and n is the number of particles per unit volume. We assume an isotropic orientation distribution of particle contacts for all loading conditions, $f(\boldsymbol{\alpha}) = k/4\pi$, where k is the coordination number. As before underlined, if we had considered an evolution of the aggregate during the loading, by including changing in the coordination number and the orientation of the contacts, we would have incorporated a different expression for $f(\boldsymbol{\alpha})$ function of the orientation $\boldsymbol{\alpha}$ and the variation of the average number of contacts. Here $f(\boldsymbol{\alpha})$ is assumed to be constant and, therefore, it will not influence the integrations that we carry out.

In order to phrase the problem in a more compact form we introduce two alternative parameters b and c such that

$$b = \Delta - 2\gamma = -3E_{11}$$

and

$$c = 6\gamma.$$

The pressure, defined as the trace of the stress tensor, is

$$p = -\frac{1}{3} \bar{t}_{kk} = -\frac{knD}{24\pi} \int_{\Omega} P d\Omega.$$

In the isotropic initial state, in absence of shear strain, with (2) and (4), the integration leads to

$$p = -\frac{knD}{12\pi} \int_0^{2\pi} \int_0^{\pi/2} M \Delta^{3/2} \sin \theta d\theta d\varphi = \frac{kvM}{\pi D^2} \Delta_0^{3/2}, \tag{6}$$

where $v = n\pi D^3/6$ is the solid volume fraction and Δ_0 is the associated volume strain. In case of triaxial test, at fixed pressure,

$$p = -\frac{knD}{12\pi} \int_0^{2\pi} \int_0^{\pi/2} M(b + c \cos^2 \theta)^{3/2} \sin \theta d\theta d\varphi$$

and the result of the integration (Jenkins, 1988), with (6), for triaxial compression ($c \geq 0$), is

$$8\Delta_0^{3/2} = (5b + 2c)\sqrt{b + c} + \frac{3b^2}{\sqrt{c}} \log \left[\frac{\sqrt{c} + \sqrt{b + c}}{\sqrt{|b|}} \right], \quad (7)$$

while for triaxial extension ($c \leq 0$) it is

$$8\Delta_0^{3/2} = (5b + 2c)\sqrt{b + c} + \frac{3b^2}{\sqrt{-c}} \sin^{-1} \left[\sqrt{\frac{-c}{b}} \right]. \quad (8)$$

Eqs. (7) and (8) provide an implicit relation between the normalized volume change Δ/Δ_0 and the normalized shear strain c/Δ_0 at constant pressure.

2.2.2. Stress–strain relation

We define the aggregate shear stress as

$$q = -\frac{1}{2}(\bar{t}_{33} - \bar{t}_{11}),$$

where, in particular, we distinguish the contributions to the stress from the normal and tangential components of the contact force, i.e.,

$$q = q^N + q^T.$$

Using (3), the component of the shear stress contributed by the normal force is

$$q^N = \frac{3kv}{8\pi^2 D^2} \int_{\Omega} P(\alpha_3^2 - \alpha_1^2) d\Omega.$$

The result of the integration, for $b > 0$, is given by Jenkins and Strack (1993), in the case of triaxial compression ($c \geq 0$)

$$\frac{q^N}{p} = \frac{3}{64\Delta_0^{3/2}} \left[\frac{\sqrt{b+c}}{c} (3b^2 + 4bc + 4c^2) - \frac{3b^2(b+2c)}{c^{3/2}} \log \left(\frac{\sqrt{c} + \sqrt{b+c}}{\sqrt{b}} \right) \right]; \quad (9)$$

while in the case of triaxial extension, $c \leq 0$, we obtain

$$\frac{q^N}{p} = \frac{3}{64\Delta_0^{3/2}} \left[\frac{\sqrt{b+c}}{c} (3b^2 + 4bc + 4c^2) - \frac{3b^2\sqrt{-c}(b+2c)}{c^2} \sin^{-1} \sqrt{\frac{-c}{b}} \right]. \quad (10)$$

During the loading the contribution of the normal contact force to the aggregate shear stress remains entirely elastic. In contrast, the contribution of the tangential contact force exhibits inelasticity once particles begin to slide. Jenkins and Strack (1993) consider an evolution of contact displacement with the loading and the angle θ such that they distinguish regions where sliding occurs and regions where the behavior is elastic. They obtain a critical ratio of b/c associated with the first contact to slip. That is, they determine the limit of the elastic behavior of the material. Again from (3), the tangential contribution to the shear stress is

$$\frac{q^T}{p} = \frac{3kv}{8\pi^2 D^2} \int_{\Omega} (T_1\alpha_1 - T_3\alpha_3) d\Omega,$$

where, in the elastic regime, for $c \geq 0$

$$\frac{q^T}{p} = \frac{27}{4\Delta_0^{\frac{3}{2}}} \frac{(1-\nu)}{(2-\nu)} \left[\frac{\sqrt{b+c}}{48c} (3b^2 + 4bc + 4c^2) - \frac{b^2(b+2c)}{16c^{\frac{3}{2}}} \log \left(\frac{\sqrt{c} + \sqrt{b+c}}{\sqrt{b}} \right) \right], \quad (11)$$

while for $c \leq 0$

$$\frac{q^T}{p} = \frac{27}{4\Delta_0^{\frac{3}{2}}} \frac{(1-\nu)}{(2-\nu)} \left[\frac{\sqrt{b+c}}{48c} (3b^2 + 4bc + 4c^2) - \frac{b^2\sqrt{-c}(b+2c)}{16c^2} \sin^{-1} \left(\sqrt{\frac{-c}{b}} \right) \right]. \quad (12)$$

In the closed form inelastic response for q^T obtained by Jenkins and Strack (1993) and shown here in Fig. 2, we note that once sliding begins, the tangential contribution to the shear stress is relatively constant with continued strain. This is also observed in discrete simulations (e.g. Thornton and Antony, 1998). Here we do something simpler and assume that after the first slip occurs the tangential contribution to the shear stress does not change. We, therefore, employ a bilinear elastic–perfectly plastic behavior for q^T . We also note that in Eqs. (9)–(12) we have normalized the shear stress by the pressure through Eq. (6). Consequently, these expressions do not depend explicitly on the coordination number, volume fraction or diameter of the spherical particles. This directly provides relations between the stress and strain for all triaxial tests when the total strains are normalized by Δ_0 .

2.2.3. Simplified model for inelasticity

When sliding occurs between two contacting particles, the behavior of the aggregate becomes inelastic. In Jenkins and Strack (1993) the value of the polar angle θ for which sliding first occurs in triaxial compression satisfies the relation $\cot 2\theta_c^* = -\hat{\mu}$. If we restrict

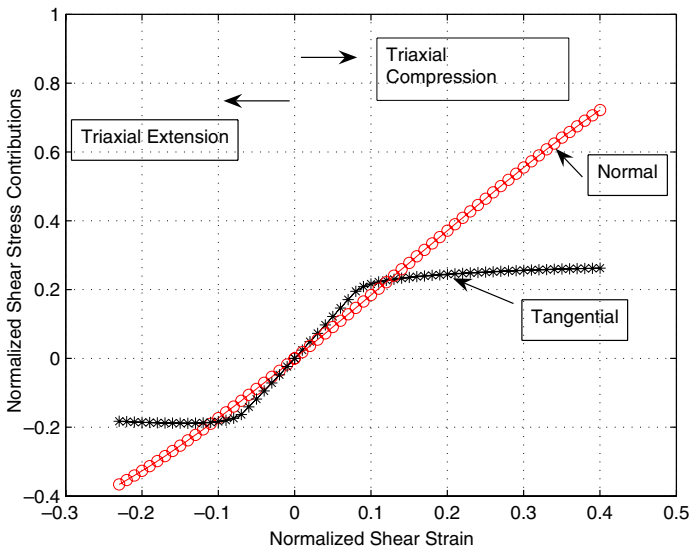


Fig. 2. Normalized shear stress (q/p) versus normalized shear strain (γ/Δ_0). Both triaxial compression and extension regimes are shown.

our attention to glass particles with coefficient of friction $\mu = 0.3$ and Poisson's ratio $\nu = 0.2$, then $\hat{\mu} = \mu(2 - \nu)/(3 - 3\nu) = 0.225$. By elementary geometry, we obtain

$$\cos 2\theta_{\text{com}}^* \equiv \frac{-\hat{\mu}}{\sqrt{1 + \hat{\mu}^2}} \simeq -\hat{\mu}.$$

Correspondingly, in triaxial extension, starting from a virgin material, $\cot 2\theta_{\text{ext}}^* = \hat{\mu}$, so

$$\cos 2\theta_{\text{ext}}^* \equiv \frac{\hat{\mu}}{\sqrt{1 + \hat{\mu}^2}} \simeq \hat{\mu}.$$

The subscript com and ext denotes parameters pertaining to triaxial compression and triaxial extension, respectively. From Eq. (5) at the onset of sliding in triaxial compression, $b = \rho c$, while for triaxial extension, $b = -\tilde{\rho} c$ where, respectively

$$\rho \equiv \frac{1 - \hat{\mu}}{2\hat{\mu}}$$

and

$$\tilde{\rho} \equiv \frac{1 + \hat{\mu}}{2\hat{\mu}}.$$

From Eqs. (7) and (8), and the above relations between b and c , we obtain the values of the normalized shear strain and normalized volume strain corresponding to the onset of sliding. For $c \geq 0$,

$$\frac{\gamma_{\text{com}}^*}{A_0} = \frac{2}{3} \left[\frac{1}{(5\rho + 2)\sqrt{\rho + 1} + 3\rho^2 \log\left(\frac{1 + \sqrt{\rho + 1}}{\sqrt{\rho}}\right)} \right]^{\frac{2}{3}} = 0.08 \tag{13}$$

and

$$\frac{A_{\text{com}}^*}{A_0} = 2(1 + 3\rho) \frac{\gamma_{\text{com}}^*}{A_0} = 0.99, \tag{14}$$

while for $c \leq 0$,

$$\frac{-\gamma_{\text{ext}}^*}{A_0} = \frac{2}{3} \left[\frac{1}{(5\tilde{\rho} + 2)\sqrt{\tilde{\rho} + 1} + 3\tilde{\rho}^2 \sin^{-1}\left(\sqrt{\frac{1}{\tilde{\rho}}}\right)} \right]^{\frac{2}{3}} = 0.07, \tag{15}$$

and

$$\frac{A_{\text{ext}}^*}{A_0} = \frac{-\gamma_{\text{ext}}^*}{A_0} (6\tilde{\rho} - 2) = 0.99. \tag{16}$$

We find, therefore, that the elastic regime for an aggregate of glass spheres, after an isotropic compression, is given by

$$-0.07 \leq \frac{\gamma}{A_0} \leq 0.08. \tag{17}$$

That is, the aggregate shows an almost symmetric behavior when compressed or extended from the initial state. Beyond this range of deformation the tangential component of the

shear stress does not surpass the limiting values reached at $\gamma_{\text{com}}^*/\Delta_0$ and $\gamma_{\text{ext}}^*/\Delta_0$. If we take $b = \rho c$ in Eq. (11) and $b = -\tilde{\rho}c$ in Eq. (12) we obtain the maximum elastic tangential contribution to the shear stress in triaxial compression and extension, respectively. This means that for each contact we take $T = \mu P^*$ where P^* is the limit value that the normal force has reached, at each orientation, for $\gamma_{\text{com}}^*/\Delta_0$ (in compression) or $\gamma_{\text{ext}}^*/\Delta_0$ (in extension).

2.2.4. Plastic deformation via frictional slip: monotonic loading

In the case of monotonic loading, we can define the plastic strain associated with sliding. Particular care must be taken as the derivation of the average strain tensor is involved. Here, we refer to the work of [Bagi \(1996\)](#) for details of that derivation. We use the final result in which the average strain tensor is given by (see also [Koenders, 1994](#); [Kruyt and Rothenburg, 1996](#); [Bagi, 2006](#))

$$E_{ij} = \frac{3}{4\pi D} \int_{\Omega} (u_i \alpha_j + u_j \alpha_i) d\Omega. \quad (18)$$

We can distinguish the part of the average strain associated with the normal component of the contact displacement from that associated with the tangential component

$$E_{ij}(\delta) = -\frac{3}{4\pi D} \int_{\Omega} 2\delta \alpha_i \alpha_j d\Omega,$$

and

$$E_{ij}(s) = \frac{3}{4\pi D} \int_{\Omega} (s_i \alpha_j + s_j \alpha_i) d\Omega,$$

respectively. Within the elastic range, given by (17), the deformation is purely elastic and the shear strain can be split as

$$\gamma^{\text{el}} = \gamma^{\text{el}}(\delta) + \gamma^{\text{el}}(s),$$

which coincides with the total shear strain applied. Each contribution to the elastic shear strain can be evaluated

$$\begin{aligned} \gamma^{\text{el}}(\delta) &= -\frac{1}{2} [E_{33}(\delta) - E_{11}(\delta)] \\ &= \frac{1}{4\pi} \int_0^{2\pi} \int_0^{\pi/2} (b + c \cos^2 \theta) (\cos^2 \theta - \sin^2 \theta \cos^2 \varphi) \sin \theta d\theta d\varphi = \frac{c}{15}, \end{aligned}$$

and

$$\begin{aligned} \gamma^{\text{el}}(s) &= -\frac{1}{2} [E_{33}(s) - E_{11}(s)] \\ &= \frac{3\gamma}{2\pi} \int_0^{2\pi} \int_0^{\pi/2} (\sin^2 \theta \cos^2 \theta + \sin^2 \theta \cos^2 \theta \cos^2 \varphi) \sin \theta d\theta d\varphi = \frac{c}{10}. \end{aligned}$$

At the limiting values, given by (17) the first particle slip occurs. At this limiting strain we assume all particles will slide. While this assumption appears rather strong, it is corroborated by simulations (e.g. [Thornton and Antony, 1998](#)) wherein, after a modest amount of deviatoric strain, the contribution of the tangential contact force to the deviatoric part of the stress, q^T , is nearly constant. While it is true that some contacts will still experience elastic resistance, mainly those in close proximity to direction of the greatest compressive

strain, the average behavior still results in nearly constant q^T . Therefore, while we admit that all contacts do not in fact slide, the aggregate behavior can not be distinguished from that which results when it is assumed that all contacts are sliding, an approximation that affords us significant simplification in the model development. The crude approximation introduced for the slip seems, however, to agree reasonably well with predictions by Jenkins and Strack (1993). In Appendix A we show the results of the comparison.

As the shear strain $\gamma(\delta)$ is always elastic, in triaxial compression for $\gamma \geq \gamma_c^*$, the plastic shear strain contribution is

$$\gamma_{\text{com}}^p = \gamma - \gamma^{\text{el}} = \gamma - \frac{c}{15} - \frac{3}{5}\gamma_c^* = \frac{3}{5}(\gamma - \gamma_{\text{com}}^*); \tag{19}$$

while in triaxial extension, $\gamma \leq \gamma_{\text{ext}}^*$,

$$\gamma_{\text{ext}}^p = \gamma - \gamma^{\text{el}} = \gamma - \frac{c}{15} - \frac{3}{5}\gamma_{\text{ext}}^* = \frac{3}{5}(\gamma - \gamma_{\text{ext}}^*). \tag{20}$$

This linear dependence is illustrated in triaxial compression and extension, respectively, in Fig. 3.

Within the range of elastic deformation, it is also easy to define the corresponding elastic volume change as

$$\text{tr}E_{ij} = \text{tr}E_{ij}(\delta) = -\Delta. \tag{21}$$

We note that this elastic volume change, only function of the normal contact displacement, results from microstructural anisotropy induced in the material by the applied strain through the contact forces. This dilatancy is not related to frictional-sliding or change in structure.

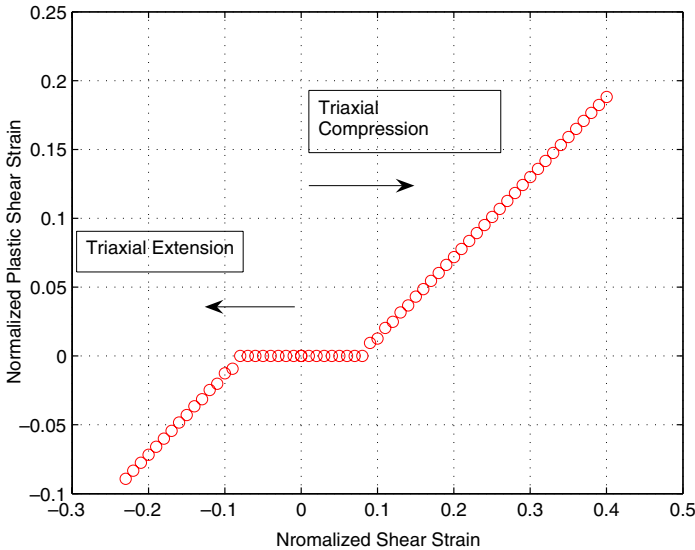


Fig. 3. Normalized plastic shear strain (γ^p/Δ_0) versus normalized total shear strain (γ/Δ_0). Both triaxial compression and extension regimes are shown.

2.2.5. Strain hardening

The relevant features of a simple model for inelastic behavior are the yield strain, the yield stress and the apparent hardening modulus, i.e., slope of the shear stress–shear strain curve after yield or slip. We seek expressions for the contributions of the normal and tangential contact forces to the shear stress given by (9)–(12), respectively, evaluated at the yield strains defined by (13)–(16), respectively. The yield shear stress can be written in triaxial compression and extension, respectively, as

$$\frac{q_{com}^*}{p} = \frac{q_{com}^{*N}}{p} + \frac{q_{com}^{*T}}{p}$$

and

$$\frac{q_{ext}^*}{p} = \frac{q_{ext}^{*N}}{p} + \frac{q_{ext}^{*T}}{p}$$

For q^N/p the limiting values are

$$\begin{aligned} \frac{q_{com}^{*N}}{p} &= \frac{9\sqrt{6}}{32} \left[\sqrt{1 + \rho}(3\rho^2 + 4\rho + 4) - 3\rho^2(\rho + 2) \log \left(\frac{1 + \sqrt{1 + \rho}}{\sqrt{\rho}} \right) \right] \left(\frac{\gamma_{com}^*}{\Delta_0} \right)^{\frac{3}{2}} \\ &= 0.148 \end{aligned} \tag{22}$$

and

$$\frac{q_{ext}^{*N}}{p} = \frac{9\sqrt{6}}{32} \left[-\sqrt{\tilde{\rho} - 1}(3\tilde{\rho}^2 - 4\tilde{\rho} + 4) + 3\tilde{\rho}^2(\tilde{\rho} - 2) \sin^{-1} \left(\sqrt{\frac{1}{\tilde{\rho}}} \right) \right] \left(\frac{-\gamma_{ext}^*}{\Delta_0} \right)^{\frac{3}{2}} = -0.122;$$

while for q^T/p

$$\begin{aligned} \frac{q_{com}^{*T}}{p} &= \frac{3\sqrt{6}}{8} \left[\sqrt{\rho + 1}(3\rho^2 + 4\rho + 4) - 3\rho^2(\rho + 2) \log \left(\frac{1 + \sqrt{1 + \rho}}{\sqrt{\rho}} \right) \right] \left(\frac{\gamma_{com}^*}{\Delta_0} \right)^{3/2} \\ &= 0.197 \end{aligned} \tag{23}$$

and

$$\frac{q_{ext}^{*T}}{p} = \frac{3\sqrt{6}}{8} \left[\sqrt{1 - \tilde{\rho}}(3\tilde{\rho}^2 - 4\tilde{\rho} + 4) - 3\tilde{\rho}^2(2 - \tilde{\rho}) \sin^{-1} \left(\sqrt{\frac{1}{\tilde{\rho}}} \right) \right] \left(\frac{-\gamma_{ext}^*}{\Delta_0} \right)^{3/2} = -0.163.$$

Because we assume that q^T/p is constant outside the limits (17), only q^N/p will vary with γ^p . Therefore, in triaxial compression and extension, we derive the relation between q^N/p and γ^p/Δ_0 . We refer to Appendix B for the details. In triaxial compression, from Eqs. (7), (9), and (19), with $\gamma \geq \gamma_{com}^*$

$$\begin{aligned} 8\Delta_0^{3/2} &= \left[5\Delta + 2 \left(\frac{5}{3} \gamma^p + \gamma_{com}^* \right) \right] \sqrt{\Delta + 4 \left(\frac{5}{3} \gamma^p + \gamma_{com}^* \right)} + \frac{3 \left[\Delta - 2 \left(\frac{5}{3} \gamma^p + \gamma_{com}^* \right) \right]^2}{\sqrt{6 \left(\frac{5}{3} \gamma^p + \gamma_{com}^* \right)}} \\ &\times \log \left[\frac{\sqrt{6 \left(\frac{5}{3} \gamma^p + \gamma_{com}^* \right)} + \sqrt{\Delta + 4 \left(\frac{5}{3} \gamma^p + \gamma_{com}^* \right)}}{\sqrt{\Delta - 2 \left(\frac{5}{3} \gamma^p + \gamma_{com}^* \right)}} \right] \end{aligned}$$

and

$$\frac{q_{\text{com}}^{\text{N}}}{p} = h_{\text{com}} \frac{\gamma^p}{\Delta_0}, \tag{24}$$

where, again, in case of glass spheres

$$h_{\text{com}} \simeq 3.1. \tag{25}$$

In the same way, with (8), (10), and (20), in triaxial extension

$$\frac{q_{\text{ext}}^{\text{N}}}{p} = h_{\text{ext}} \frac{\gamma^p}{\Delta_0},$$

where

$$h_{\text{ext}} \simeq 2.9.$$

In Fig. 4 we plot the relation between the normalized shear stress and the normalized plastic shear strain, respectively in triaxial compression and extension.

2.2.6. Plastic volume strain: unloading regime

As underlined in Jenkins and Strack (1993), and, indicated in Eq. (21) here, it follows from the kinematic assumption in (1) that there is not apparently volume change associated with the tangential part of the displacement. Moreover, during the loading, while it is possible to define a plastic shear strain associated with sliding, there is not an analogous expression for the plastic volume change. Nevertheless, because particles slide during the loading, when we unload we first have an elastic resistance among grains and then a reverse slip occurs. As consequence the unloading path, in a stress- strain curve, will not follow the previous loading. We define, therefore, the plastic volume change as the

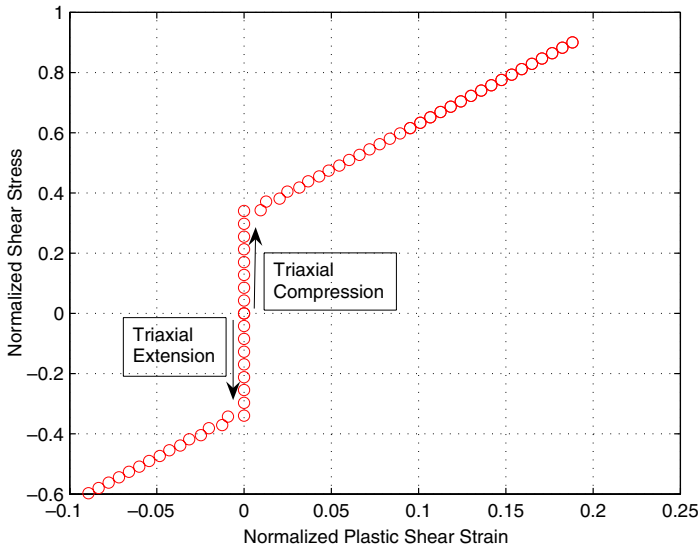


Fig. 4. Normalized shear stress (q/p) versus normalized plastic shear strain (γ^p/Δ_0). Both triaxial compression and extension regimes are shown.

amount of volume locked in the material after the material is triaxially compressed and subsequently unloaded to zero shear stress. Before we provide more details for the definition of the plastic volume change and in order to obtain a simple analytical expression for **it**, we first introduce some simplifications.

From Figs. 2 and 4, it is reasonable to approximate a shear response for which the yield strains in compression and extension are equal ($\gamma^* = -\gamma_{\text{ext}}^* = \gamma_{\text{com}}^*$) and the elastic modulus, \bar{G} , and the hardening modulus \bar{H} of the aggregate are constant. Therefore, for $\gamma \leq \gamma_{\text{com}}^*$,

$$\frac{q}{p} = \frac{\bar{G}}{A_0} \gamma;$$

while for $\gamma \geq \gamma_{\text{c}}^*$, using (19),

$$\frac{q}{p} = \frac{\bar{G}}{A_0} (\gamma - \gamma^p) = \bar{G} \frac{\gamma_{\text{com}}^*}{A_0} + \frac{2\bar{G}}{5} \frac{(\gamma - \gamma_{\text{com}}^*)}{A_0}.$$

Consequently, the hardening modulus is

$$\bar{H} = \frac{2}{5} \bar{G}. \quad (26)$$

With these simplifying assumptions, we first consider the case in which we shear the material up to a value γ_{max}/A_0 with the corresponding shear stress $q_{\text{max}}/p \leq 2\bar{G}\gamma_{\text{com}}^*/A_0$. Upon unloading, the material remains elastic for reverse strain equal to $2\gamma^*/A_0$ after which reverse slip begins. That is, the elastic region obtained in the virgin state in compression and extension provides the range of elastic deformation in reverse loading. In Appendix C, we provide a comparison between an incremental model based upon a more complex description of contact sliding during loading and unloading and this simplified model. We note that, within a reasonable approximation, the two models produce results that are in agreement. That is, the assumption of kinematic rather than isotropic hardening is borne out by a fully incremental formulation and experimental results (e.g. Tatsuoka and Ishihara, 1974). It, therefore, seems reasonable to adopt this simplification in this regime of deformation. In this context the normalized stress, in case of unloading, is

$$\frac{q}{p} = \bar{G} \frac{\gamma^*}{A_0} + \bar{H} \frac{(\gamma_{\text{max}} - \gamma^*)}{A_0} - \bar{G} \frac{(\gamma_{\text{max}} - \gamma)}{A_0}.$$

If we define γ_{R} as the residual shear strain associated with zero total shear stress upon unloading, then

$$\bar{G}\gamma^* + \bar{H}(\gamma_{\text{max}} - \gamma^*) - \bar{G}(\gamma_{\text{max}} - \gamma_{\text{R}}) = 0.$$

With Eq. (26) the residual strain associated with the unloaded state is

$$\gamma_{\text{R}} = \frac{3}{5}(\gamma_{\text{max}} - \gamma^*) = \gamma^p.$$

That is, when we unload from $q_{\text{max}}/p \leq 2\bar{G}\gamma^*/A_0$ the residual strain, γ_{R} , coincides with the plastic strain γ^p accumulated during the previous loading.

If during the loading we reach the value $q_{\text{max}}/p \geq 2\bar{G}\gamma^*/A_0$ then the unloading regime necessary to reaches the zero shear stress will involve reverse slip

$$\frac{q}{p} = \bar{G} \frac{\gamma^*}{A_0} + \bar{H} \frac{(\gamma_{\text{max}} - \gamma^*)}{A_0} - 2\bar{G} \frac{\gamma^*}{A_0} - \bar{H} \frac{(\gamma_{\text{max}} - 2\gamma^* - \gamma)}{A_0}$$

and, in particular, for the shear stress relaxed to zero, $\gamma = \gamma_R$,

$$\gamma_R = \frac{3}{2}\gamma^*$$

which is constant, irrespective of the value of q_{\max}/p reached after the limit of $2\bar{G}\gamma^*/\Delta_0$. This simple description of loading and unloading behavior of the material is illustrated in Fig. 5. The model considers a fixed range of elastic deformation that is obtained in its virgin state from triaxial compression and extension test.

For the purposes of identifying a simple expression for the plastic volume change, we now restrict our attention to the case when the normalized shear stress does not exceed the value $2\bar{G}\gamma^*/\Delta_0$. The material will relax to a zero shear stress without experiencing any reverse slip. This is, in general, not rigorously true, as in the unloading regime, some particle contacts may, indeed, experience some reverse sliding. Here, however, from the qualitative point of view and because we are focusing on strains prior to contact deletion, we restrict our attention to purely elastic unloading of the aggregate to $q/p = 0$. This corresponds directly to unloading from maximum normalized shear stresses that do not exceed $2\bar{G}\gamma_{\text{com}}^*/\Delta_0$; then the corresponding residual strain is precisely the accumulated plastic strain in the loading regime and the plastic volume strain in the aggregate is defined as the volume “locked” in the material when q/p is relaxed to zero. That is, in this range of deformation, because we do not have change in structure, the volume strain is only related to the normal component of the contact displacement, Eq. (21). Thereby, unloading to $q/p = 0$, does not correspond to both $q^N/p = 0$ and $q^T/p = 0$ simultaneously. In particular, $q^N/p \neq 0$ implies that from Eq. (2) there are some contacts for which δ has not recovered to its initial value $D\Delta_0/6$.

With $\gamma = \gamma^p$, we write, from Eq. (7)

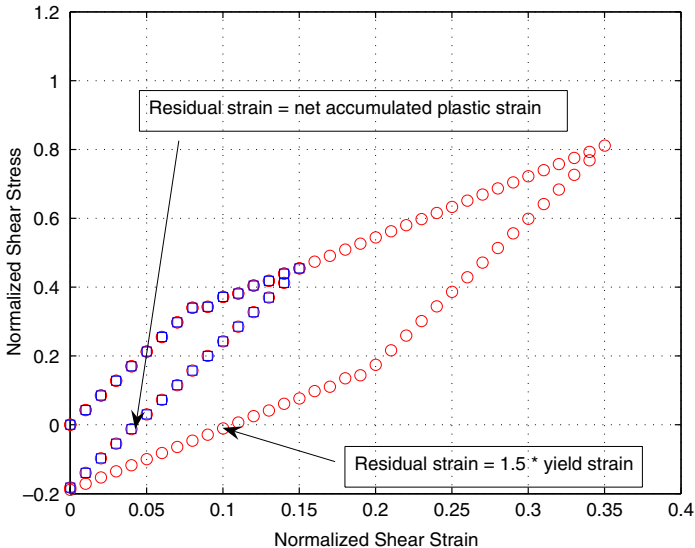


Fig. 5. Normalized shear stress (q/p) versus normalized shear strain (γ/Δ_0): the aggregate’s residual strain varies with the starting point for unloading.

$$8\Delta_0^{3/2} = (5\hat{b} + 2\hat{c})\sqrt{\hat{b} + \hat{c}} + \frac{3\hat{b}^2}{\sqrt{\hat{c}}} \log \left[\frac{\sqrt{\hat{c}} + \sqrt{\hat{b} + \hat{c}}}{\sqrt{\hat{b}}} \right] \quad (27)$$

with $\hat{c} = 6\gamma^p$ and $\hat{b} = \Delta^p + \Delta_0 - 2\gamma^p$ (where for $\gamma^p = 0$ we have $\Delta^p = 0$). For each value of the strain $\gamma \geq \gamma^*$, (27) determines a corresponding irreversible amount of plastic volume strain that will remain in the unloaded state.

2.2.7. Yield function

We have now sufficient information to write the expressions for the yield and potential functions. In particular for the former, at first yield

$$\frac{q^*}{p} = \frac{q^N}{p}(\gamma^*) + \frac{q^T}{p}(\gamma^*).$$

Then, using (22) and (23) in the q - p plane,

$$q^* = \xi p \quad (28)$$

with $\xi = 0.345$. Beyond yield, for $\gamma \geq \gamma^*$ and

$$q = q^* + q_{\text{com}}^N(\gamma^p),$$

where $\gamma^p = 3(\gamma - \gamma_{\text{com}}^*)/5$ and, from Eqs. (24) and (25),

$$q = \left(\xi + h_{\text{com}} \frac{\gamma^p}{\Delta_0} \right) p. \quad (29)$$

These describe yield lines in the q - p plane that provide the Mohr–Coulomb yield criterion. In our model, material hardening depends upon the relation between q^N/p and γ^p/Δ_0 .

2.2.8. Potential function

It is well-known that granular materials that exhibit dilatancy are described by a non-associated flow rule. In this case, the yield function is distinct from the potential function. Our goal is to derive an expression for the potential function starting from the micro-mechanics in the context of the simple model presented here. The potential function g is a function of the shear stress q and the pressure p . In the q - p plane, curves with g constant are obtained by

$$dg = 0 \Rightarrow \frac{\partial g}{\partial q} dq + \frac{\partial g}{\partial p} dp = 0. \quad (30)$$

By definition, the direction of the incremental plastic strain is orthogonal to the potential function. By decomposing the incremental plastic strain into a plastic shear component and a plastic volume component, we obtain

$$\frac{\partial g}{\partial q} = \lambda \frac{d\gamma^p}{d\gamma}$$

and

$$\frac{\partial g}{\partial p} = \lambda \frac{d\Delta^p}{d\gamma},$$

where λ is a constant. Eq. (30), with the above expressions, becomes

$$\frac{d\gamma^p}{d\gamma} dq + \frac{d\Delta^p}{d\gamma} dp = 0$$

or, equivalently,

$$\frac{dq}{dp} = -\frac{d\Delta^p}{d\gamma^p}. \tag{31}$$

This equation provides the relation between dilatancy and stress. Eq. (27) is an implicit relation between plastic shear strain and plastic volume change. Here we adopt the following quadratic fit:

$$\frac{\Delta^p}{\Delta_0} = \beta \left(\frac{\gamma^p}{\Delta_0} \right)^2. \tag{32}$$

The initial slope is zero; that is, at $\gamma^p = 0$, there is no plastic volume change. We show in Fig. 6 that this approximation is excellent for $\beta = -0.8$.

From Eq. (32), we obtain a much simpler expression for the ratio of the plastic volume strain increment to the plastic shear strain increment

$$\frac{d\Delta^p}{d\gamma^p} = 2\beta \frac{\gamma^p}{\Delta_0}. \tag{33}$$

Using Eqs. (29) and (33), we obtain

$$\frac{d\Delta^p}{d\gamma^p} = \frac{2\beta}{h_c} \left(\frac{q}{p} - \xi \right).$$

Therefore, with (31), in the q - p plane, the curves of the potential function are represented by

$$\frac{dq}{dp} = \kappa_1 \frac{q}{p} + \kappa_2,$$

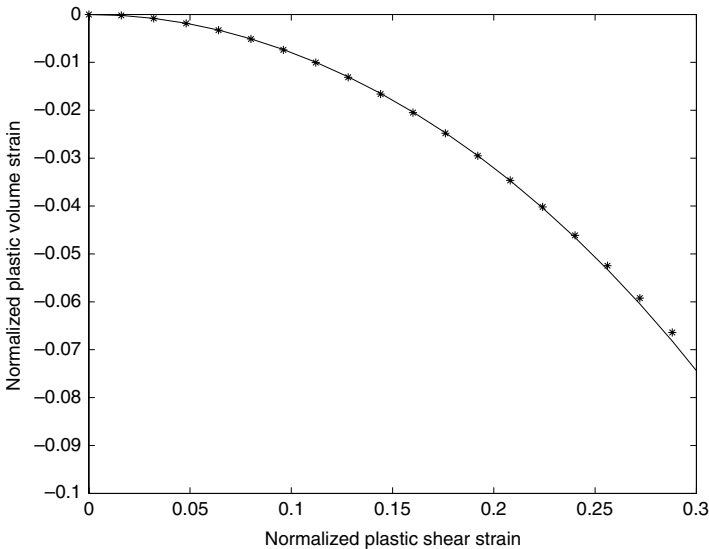


Fig. 6. Normalized plastic volume strain (Δ^p/Δ_0) versus normalized plastic shear strain (γ^p/Δ_0): comparison between analytical solution and a quadratic approximation function with $\beta = -0.8$.

with $\kappa_1 = -2\beta/h_{\text{com}}$ and $\kappa_2 = 2\beta\xi/h_{\text{com}}$. The integral of these is given by

$$q = Cp^{\kappa_1} - \frac{\kappa_2}{\kappa_1 - 1}p.$$

In the q - p plane, we can now plot both the yield lines given by the Mohr–Coulomb criterion and the potential function. The shear stress at first yield is $q^* = \xi p$, determining the constant C

$$C = \left(\xi + \frac{\kappa_2}{\kappa_1 - 1} \right) p^{1-\kappa_1}.$$

The expression for the potential function is then

$$g \equiv q - \left(\xi + \frac{\kappa_2}{\kappa_1 - 1} \right) \hat{p}^{1-\kappa_1} p^{\kappa_1} + \frac{\kappa_2}{\kappa_1 - 1} p = 0,$$

where \hat{p} is the value of the expression in which the potential function intersects the first yield line. In Fig. 7, we plot both a family of yield functions and potential functions, in case of glass spheres, and explicitly label the line that corresponds to the onset of yielding. Below the first yield line (dashed line), given by Eq. (28), the material behaves elastically. Note, the plastic potential curves will pass through the origin and collapse to the first yield line. This line intersects the potential functions at maximum values where their slope vanishes, implying that the incremental strain vector is parallel to the q axis. That is, there is no dilatancy in this virgin state. Each successive yield line is defined for a given amount of accumulated plastic strain and, therefore, we define for each yield line one direction for the incremental plastic strain vector. Within the adopted approximation, it is not the total shear stress, but only its normal contribution that provides the slope of the yield function. We also see that, beyond first yield, the projection of the incremental plastic strain vector on the p axis is negative. This implies a negative plastic volume strain or dilatancy.

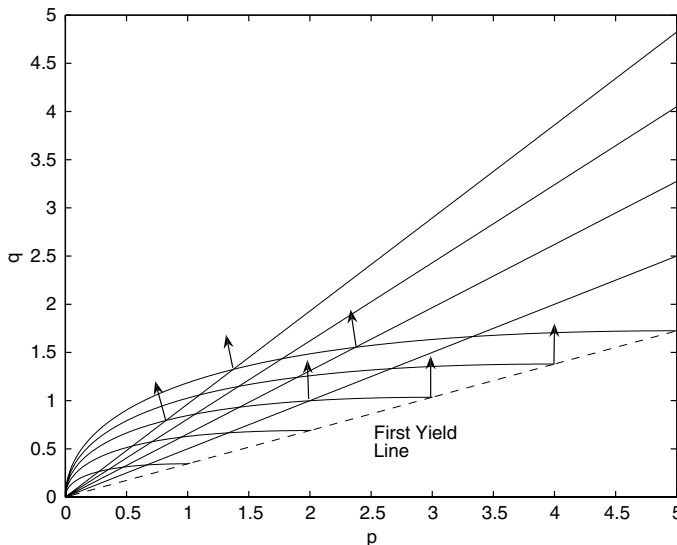


Fig. 7. Family of straight yield lines and potential curves.

3. Conclusions

We have provided a relatively simple model for the response of a random aggregate of spherical grains that interact through sustained contact forces in triaxial compression and extension. The model is a simplified approximation to a complete analytic integration of the evolving contact forces. The contact displacement between particles is assumed to be given by the average strain leading to predictions of aggregate shear stress that represent an upper bound to the real material response. However, in this framework, we derive closed-form expressions for the yield strain, yield stress, hardening moduli, volume change, plastic shear and volume strains, yield and potential functions. In particular we have emphasized qualitative features of this material from a micro-mechanical point of view, underlining those aspects that are crucial to understanding the inelastic response of the material.

Acknowledgements

The authors are grateful to Prof. J.T. Jenkins (Cornell University) for his suggestions and stimulating discussions during the preparation of the manuscript. L. La Ragione thanks grant from M.I.U.R-COFIN 2005, G.N.F.M. and PST-Regione Puglia.

Appendix A. An approximation for accumulated plastic strain

The aggregate shear stress response is given for both triaxial compression and triaxial extension by adopting a full integrated expression from [Jenkins and Strack \(1993\)](#). For both compression and extension, it is observed that the contribution of tangential contact forces to the aggregate shear stress is, to good approximation, constant beyond first slip, i.e., yield (see [Fig. 2](#)).

The corresponding assumption is that the contribution of the tangential contact displacement to the elastic shear strain is constant after yield and, therefore, a simple expression for plastic shear strain is obtained (Eqs. (19) and (20)). An illustration of this simplification for the plastic shear strain is shown in [Fig. 8](#) along with the predictions of the full integrated model.

The slight increase in the tangential contribution to the aggregate shear stress indicates that the elastic strain associated with the tangential contact displacement is not exactly constant after yield. It is this small amount of elastic strain that accounts for the roughly 5% discrepancy between the plastic shear strain predicted by the full integrated model and the simplification offered here.

Appendix B. A simplified model of strain hardening

For both compression and extension, it is observed that the contribution of tangential contact forces to the aggregate shear stress is, to a good approximation, constant beyond first slip, i.e., yield. In addition, the contribution of normal contact forces to the aggregate shear stress remains purely elastic and, to good approximation, varies linearly with the normalized strain.

It is then reasonable to re-cast Eq. (9) isolating a term linear in the shear variable γ , giving

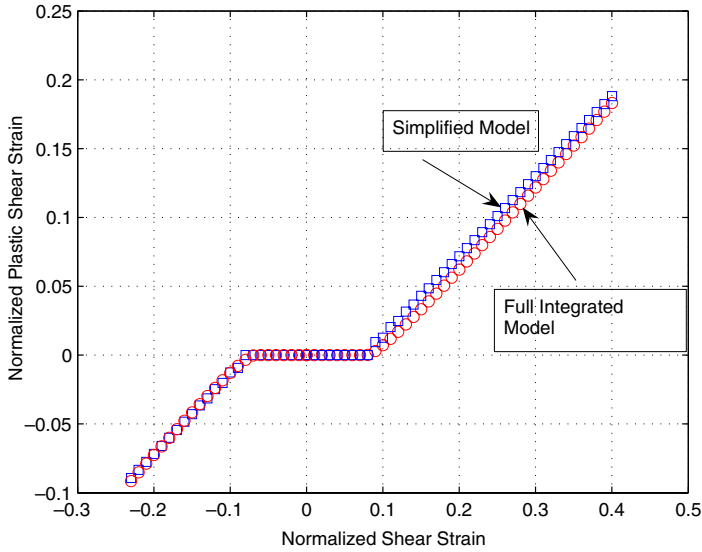


Fig. 8. Comparison between the simplified model and the fully integrated solution.

$$\frac{q^N}{p} = \frac{9}{32} \sqrt{\frac{c}{\Delta_0}} \left[\sqrt{1 + \frac{b}{c}} \left(3 \frac{b^2}{c^2} + 4 \frac{b}{c} + 4 \right) - 3 \frac{b^2}{c^2} \left(\frac{b}{c} + 2 \right) \log \left(\frac{1 + \sqrt{1 + \frac{b}{c}}}{\sqrt{\frac{b}{c}}} \right) \right] \frac{\gamma}{\Delta_0}$$

$$= \mathcal{R} \frac{\gamma}{\Delta_0},$$

where \mathcal{R} , to a good approximation, remains constant (see Fig. 2). For simplicity, we evaluate \mathcal{R} at first yield, where ρ is the critical ratio at first slip and $c = 6\gamma_c^*$, giving with (13)

$$\mathcal{R} = \frac{9}{32} \left[\sqrt{1 + \rho} (3\rho^2 + 4\rho + 4) - 3\rho^2 (\rho + 2) \log \left(\frac{1 + \sqrt{1 + \rho}}{\sqrt{\rho}} \right) \right]$$

$$\times \left[\frac{8}{(5\rho + 2)\sqrt{\rho + 1} + 3\rho^2 \log \left(\frac{1 + \sqrt{\rho + 1}}{\sqrt{\rho}} \right)} \right]^{1/3} \cong 1.85.$$

Finally, using (19)

$$\frac{q^N}{p} = \mathcal{R} \frac{\gamma}{\Delta_0} = \mathcal{R} \left(\frac{\gamma_c^*}{\Delta_0} + \frac{5}{3} \frac{\gamma^p}{\Delta_0} \right) = \frac{q_{\text{com}}^*}{p} + \frac{5}{3} \mathcal{R} \frac{\gamma^p}{\Delta_0} = \frac{q_{\text{com}}^*}{p} + 3.08 \frac{\gamma^p}{\Delta_0}.$$

Applying an identical linearization in triaxial extension, results in the expression

$$\frac{q_{\text{ext}}^N}{p} = \mathcal{J} \frac{\gamma}{\Delta_0},$$

with

$$\mathcal{J} = \frac{9}{32} \left[-\sqrt{\tilde{\rho}-1}(3\tilde{\rho}^2 - 4\tilde{\rho} + 4) + 3\tilde{\rho}^2(\tilde{\rho} - 2) \sin^{-1} \sqrt{\frac{1}{\tilde{\rho}}} \right] \times \left[\frac{8}{(5\tilde{\rho} - 2)\sqrt{\tilde{\rho}-1} + 3\tilde{\rho}^2 \sin^{-1} \sqrt{\frac{1}{\tilde{\rho}}}} \right]^{1/3} \cong 1.74.$$

Giving, with Eq. (20),

$$\frac{q_{\text{ext}}^{\text{N}}}{p} = \mathcal{J} \frac{\gamma}{\Delta_0} = \frac{q_{\text{ext}}^{\text{N}}}{p} = \mathcal{J} \left(\frac{\gamma_{\text{ext}}^*}{\Delta_0} + \frac{5}{3} \frac{\gamma^p}{\Delta_0} \right) = \frac{q_{\text{ext}}^{\text{N}}}{p} + \frac{5}{3} \mathcal{J} \frac{\gamma^p}{\Delta_0} = \frac{q_{\text{ext}}^{\text{N}}}{p} + 2.9 \frac{\gamma^p}{\Delta_0}.$$

Appendix C. Motivation for a simplified model of unloading

In this work, we have associated the onset of aggregate yielding with this first slip between particles. Because the yield point is relatively “sharp” when loading the material in triaxial compression, associating aggregate yield with a critical ratio of strains b/c , as is done in Section 2.2.3 is reasonable.

The case of unloading and subsequently reverse loading the aggregate can be carried out in a manner strictly analogous to the case of monotonic loading considered by Jenkins and Strack (1993). Using a corresponding reverse slip criterion, further parameterized by the maximum shear strain on forward loading, the shear stress response can be directly computed. Upon unloading to reverse yielding, we observe three specific characteristics of the material response: first, the point of first reverse slip is a function of the amount of pre-strain prior to reversal; second, the yielding on reverse sliding is more gradual, i.e., the strain transient of the yielding results in a broadened “knee” of the stress–strain

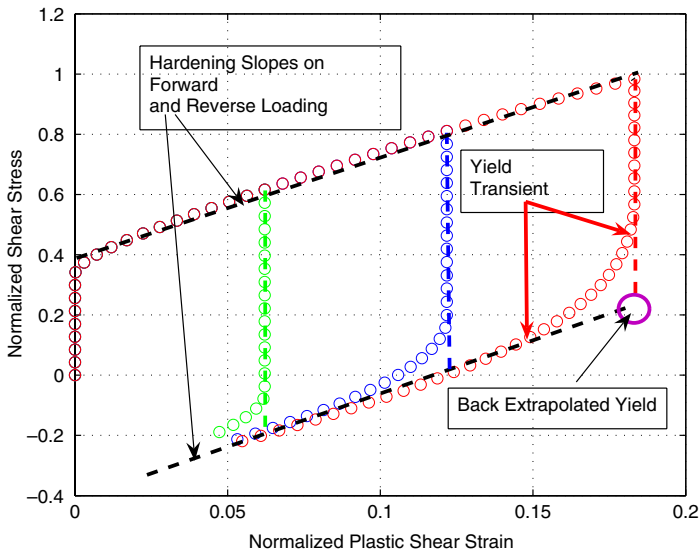


Fig. 9. Loading and unloading using a reverse slip functional (circles) along with a simplified model (dashed lines).

response and third, eventually, the stress strain response saturates to a constant hardening slope in reverse sliding that is nearly identical to that for forward loading. These characteristic behaviors are illustrated in Fig. 9. If we are interested in only this so-called long strain asymptotic behavior, the stress response can be approximated as bilinear with constant elastic slopes within an elastic region bounded by the original virgin state of the material and constant inelastic hardening slopes beyond yield. If one draws these extrapolated, straight line segments, the elastic regime, to a very good approximation, appears bounded by a shear stress difference of $2\bar{G}_{\text{com}}^*/\Delta_0$. With this proposed simplification, it is possible to motivate relatively simple forms for the aggregate inelastic stress response, the plastic volume change and plastic potential functions.

References

- Bagi, K., 1996. Stress and strain in granular assemblies. *Mechanics of Materials* 22, 165–177.
- Bagi, K., 2006. Analysis of microstructural strain tensor for granular assemblies. *International Journal of Solids and Structures* 43, 3166–3184.
- Chang, C.S., Hicher, P.Y., 2005. An elasto-plastic model for granular materials with microstructural consideration. *International Journal of Solids and Structures* 42, 4258–4277.
- Elata, D., Berryman, J.G., 1996. Contact force–displacement laws and the mechanical behavior of random packs of identical spheres. *Mechanics of Materials* 24, 229–240.
- Hashiguchi, K., Tsutsumi, S., 2007. Gradient plasticity with the tangential-subloading surface model and the prediction of shear-band thickness of granular materials. *International Journal of Plasticity* 23, 767–797.
- Jenkins, J.T., 1988. Volume change in small strain axisymmetric deformations of a granular material. In: Satake, M., Jenkins, J.T. (Eds.), *Micromechanics of Granular Materials*. Elsevier, Amsterdam, pp. 245–252.
- Jenkins, J.T., 1997. In elastic behavior of random arrays of identical spheres. In: Fleck, N.A. (Ed.), *Mechanics of Granular and Porous Materials*. Kluwer, Amsterdam, pp. 11–22.
- Jenkins, J.T., Strack, O.D.L., 1993. Mean-field inelastic behavior of random arrays of identical spheres. *Mechanics of Materials* 16, 25–33.
- Koenders, M.A., 1987. The incremental stiffness of an assembly of particles. *Acta Mechanica* 70, 31–49.
- Koenders, M.A., 1994. Least squares methods for the mechanics of nonhomogeneous granular assemblies. *Acta Mechanica* 106, 23–40.
- Kruyt, N.P., Rothenburg, L., 1996. Micromechanical Definition of the Strain Tensor for Granular Materials. *Journal of Applied Mechanics* 118, 706–711.
- Liao, C.L., Chang, T.P., Young, D., Chang, C.S., 1997. Stress–strain relationship for granular materials based on hypothesis of best fit. *International Journal of Solids and Structures* 34 (31–32), 4087–4100.
- Love, A.E.H., 1942. *A Treatise on the Mathematical Theory of Elasticity*. Note B. Cambridge University Press, Cambridge.
- Mindlin, R.D., Deresiewicz, H., 1953. Elastic spheres in contact under varying oblique forces. *Journal of Applied Mechanics* 20, 327–344.
- Misra, A., Chang, C.S., 1993. Effective elastic moduli of heterogeneous granular solids. *International Journal of Solids and Structures* 30, 2547–2566.
- Nemat-Nasser, S., Zhang, J., 2002. Constitutive relations for cohesionless frictional granular material. *International Journal of Plasticity* 18, 531–547.
- Nicot, F., Darve, F., 2005. RNVO Group: Natural Hazards and Vulnerability of Structures . A multi-scale approach to granular materials. *Mechanics of Materials* 37, 980–1006.
- Nicot, F., Darve, F., 2006. Micro-mechanical investigation of material instability in granular assemblies. *International Journal of Solids and Structures* 43, 3569–3595.
- Nicot, F., Darve, F., 2007. Basic features of plastic strains: From micro-mechanics to incrementally nonlinear model. *International Journal of Plasticity* 23, 1555–1588.
- Nicot, F., Sibille, L., Donze, F., Darve, F., 2007. From microscopic to macroscopic second-order work in granular assemblies. *Mechanics of Materials* 39, 664–684.
- Tatsuoka, F., Ishihara, K., 1974. Drained deformation of sand under cyclic stresses reversing direction. *Soils and Foundations* 14, 63–76.

- Thornton, C., Antony, S.J., 1998. Quasi-static deformation of particulate media. *Philosophical Transactions of the Royal Society of London Series A* 356, 2763–2782.
- Tsutsumi, S., Hashiguchi, K., 2005. General non-proportional loading behavior of soils. *International Journal of Plasticity* 21, 1941–1969.
- Vardoulakis, I., Aifantis, E.C., 1991. A gradient flow theory of plasticity for granular media. *Acta Mechanica* 87, 197–217.
- Zhu, H., Mehrabadi, M.M., Massoudi, M., 2006a. Incorporating the effects of fabric in the dilatant double shearing model for planar deformation of granular materials. *International Journal of Plasticity* 22, 628–653.
- Zhu, H., Mehrabadi, M.M., Massoudi, M., 2006b. Three-dimensional constitutive relations for granular materials based on the dilatant double shearing mechanism and the concept of fabric. *International Journal of Plasticity* 22, 826–857.